JOURNAL OF BACTERIOLOGY, Dec. 1998, p. 6625–6634 Vol. 180, No. 24
0021-9193/98/$04.00+0

Topological Analysis of the Aerobic Membrane-Bound Formate Dehydrogenase of *Escherichia coli*

STÉPHANE BENOIT, HAFID ABAIBOU,† AND MARIE-ANDRÉE MANDRAND-BERTHELOT*

Laboratoire de Génétique Moléculaire des Microorganismes et des Interactions Cellulaires, CNRS UMR 5577, Institut National des Sciences Appliquées, F-69621 Villeurbanne Cedex, France

Besides formate dehydrogenase N (FDH-N), which is involved in the major anaerobic respiratory pathway in the presence of nitrate, *Escherichia coli* synthesizes a second isoenzyme, called FDH-O, whose physiological role is to ensure rapid adaptation during a shift from aerobiosis to anaerobiosis. FDH-O is a membrane-bound enzyme complex composed of three subunits, α (FdoG), β (FdoH), and γ (FdoI), which exhibit high sequence similarity to the equivalent polypeptides of FDH-N. The topology of these three subunits has been studied by using *blaM* (β-lactamase) gene fusions. A collection of 47 different randomly generated Fdo-BlaM fusions, 4 site-specific fusions, and 3 sandwich fusions were isolated along the entire sequence of the three subunits. In contrast to previously reported predictions from sequence analysis, our data suggested that the αβ catalytic dimer is located in the cytoplasm, with a C-terminal anchor for β protruding into the periplasm. As expected, the γ subunit, which specifies cytochrome *b*, was shown to cross the cytoplasmic membrane four times, with the N and C termini exposed to the cytoplasm. Protease digestion studies of the ^{35}S-labelled FDH-O heterotrimer in spheroplasts add further support to this model. Consistently, prior studies regarding the bioenergetic function of formate dehydrogenase provided evidence for a mechanism in which formate is oxidized in the cytoplasm.

Escherichia coli synthesizes two formate-to-nitrate respiratory chains which allow energy conservation via oxidative phosphorylation, depending on the physiological growth conditions. Under anaerobic conditions in the presence of nitrate, a major inducible pathway, including formate dehydrogenase N (FDH-N) linked by a quinone to nitrate reductase A (NAR-A), catalyzes the proton-translocating oxidation of formate at the expense of nitrate reduction to nitrite (13, 15). In contrast, a second minor pathway, which consists of the corresponding FDH-O (also called FDH-Z) and NAR-Z membrane-bound isoenzymes, is also present under aerobic conditions and only slightly induced by nitrate (1, 21, 36). A physiological role of this constitutive pathway would be to ensure rapid adaptation during a sudden shift from aerobiosis to anaerobiosis before synthesis of the inducible pathway reaches a sufficient level (1).

From sequence predictions and by analogy with FDH-N, the FDH-O isoenzyme is a complex of three subunits, α (FdoG; 113 kDa), β (FdoH; 33 kDa), and γ (FdoI; 25 kDa) (35). The α subunit, comprising 1,017 amino acids, corresponds to the selenomolybdenum polypeptide that contains the catalytic site of formate oxidation; the β subunit is an electron transfer unit of 301 amino acids which harbors four [4Fe-4S] centers; and the γ subunit, which is composed of 203 amino acids, specifies the cytochrome *b* apoprotein. These three subunits exhibit a considerable degree of identity with those of FDH-N, as predicted from inspection of the respective *fdoGHI* and *fdnGHI* operon sequences (6, 35). The α and β subunits exhibited up to 75% identity, whereas the γ subunits were 45% identical. Moreover, both FDH enzymes display a formate phenazine methosulfate (PMS) oxidoreductase (FDH-PMS) activity and are recognized by antibodies specific to FDH-N, which confirms the functional relationship between the two enzymes (36).

Previous studies have shown that FDH-N is a membrane-bound enzyme complex (16), but orientations of the different subunits with respect to the cytoplasmic membrane have not been clearly determined. In particular, the α subunit of FDH-N was first proposed to span the cytoplasmic membrane on the basis of studies using non-membrane-permeant reagents to probe spheroplasts and right-side-out membrane vesicles (18). Its location was subsequently determined to be in the periplasm after the nucleotide sequence of the relevant *fdnG* gene had been reported, given the presence of an RRXFXK motif conserved in the N-terminal part of precursor polypeptides of periplasmic proteins binding redox cofactors (6, 7).

To investigate the membrane organization of the FDH-O subunits, we decided to use a gene fusion technique approach which has been successfully used to analyze the topological arrangement of proteins within the bacterial cytoplasmic membrane. Among the three reporter enzymes of *E. coli*, the periplasmic alkaline phosphatase PhoA (28) and β-lactamase BlaM (12) and the cytoplasmic β-galactosidase LacZ (39), we chose to construct in-frame fusions with the β-lactamase, which functions as a monomer, constitutes a more robust reporter, and presents the advantage of allowing detection of fusions on both sides of the membrane. Indeed, if the BlaM protein lacking its own signal sequence is fused to periplasmic portions of a membrane protein, it will confer resistance to high concentrations of ampicillin when single colonies are exposed to the antibiotic. In contrast, if BlaM is fused to cytoplasmic domains of the target protein, strains harboring the fusions are not resistant as single colonies but can be detected by resistance of patches on petri plates (12). This system has been successfully used to determine the topology of a number of cytoplasmic membrane proteins, including the anchor subunit DmsC of the *E. coli* dimethyl sulfoxide (DMSO) reductase

* Corresponding author. Mailing address: Laboratoire de Génétique Moléculaire des Microorganismes et des Interactions Cellulaires, CNRS UMR 5577, Institut National des Sciences Appliquées, Bâtiment 406, 20, avenue Albert Einstein, F-69621 Villeurbanne Cedex, France. Phone: (33) 4 72 43 81 91. Fax: (33) 4 72 43 87 14. E-mail: mandrand@insa.insa-lyon.fr.

† Present address: Department of Microbiology and Molecular Genetics, School of Medicine, Loma Linda University, Loma Linda, CA 92350.

TABLE 1. *E. coli* K-12 strains and plasmids used in this study

Strain or plasmid	Genotype or characteristics	Reference or source
Strains		
NM522	*supE thi* Δ*(lac-proAB)* Δ*(hsdMS-mcrB)5* (F′ *proAB*+ *lacI*^{q} *lacZ*Δ*M15*)	17
K38	*phoA4 pit-10 tonA22 ompF627 relA1 spoT1* λ$^+$	25
HA55	*fdo fnr*	1
MC4100-*fnr*	F$^-$ Δ*(argF-lac)U169 araD139 rpsL150 ptsF25 flbB5301 rbsR deoC1 relA1 fnr-22 zcj261*::Tn*10*	47
Plasmids		
pUC19	Ap^r *lacIPOZ′*	48
pSU9	Cm^r *lacIPOZ′*	4
pNM481	Ap^r, translational *lacZ* fusion vector	31
pBR322	Ap^r Tc^r	9
pGP1-2	Km^r, T7 gene 1 (RNA polymerase)	41
pYZ4	Km^r, cloning vector	49
pYZ5	Tc^r, *blaM* fusion vector	49
pCHAP4054	Cm^r, pUC18 derivative with a *Bam*HI/*Bam*HI *blaM* sandwich fusion cassette	O. Francetic
pHA3	Ap^r, pT7-6 carrying *fdoGHI*$^+$	1
pSH1	Km^r, pYZ4 carrying *fdoGHI*$^+$	This work
pG series	pSH1 derivatives with *fdoG′-blaM* fusions	This work
pH series	pSH1 derivatives with *fdoH′-blaM* fusions	This work
pI series	pSH1 derivatives with *fdoI′-blaM* fusions	This work
pGHI series	pSH1 derivatives with *fdoG′-blaM-fdoG′* sandwich fusions	This work

(46). However, no topological analysis of a whole multimeric redox complex has been reported to date. Our data suggest a model in which the α and β subunits of FDH-O are located in the cytoplasm and the γ subunit is anchored to the membrane by four transmembrane segments. This model, which differs significantly from predicted topology based on sequence analysis, is further supported by examination of protease accessibility of the three subunits.

MATERIALS AND METHODS

Bacterial strains, plasmids, media, and growth conditions. The *E. coli* K-12 strains and the plasmids used in this study are described in Table 1. For purposes of this study, cells were grown aerobically at 37°C on Luria-Bertani (LB) liquid or solid medium (30). Anaerobic growth was achieved in LB medium supplemented with 2 μM sodium selenite and 2 μM ammonium molybdate in 100-ml bottles filled to the top or on LB plates in GasPak anaerobic jars (BBL Microbiology Systems). For FDH-PMS assays, bacterial strains were grown aerobically in highly buffered TYEP medium adjusted to pH 6.5 (5) supplemented with sodium selenite and ammonium molybdate. When required, antibiotics were used at the following final concentrations: ampicillin, 100 μg/ml; kanamycin, 50 μg/ml; and tetracycline, 10 μg/ml.

DNA manipulations. Plasmid DNA was prepared by the alkaline lysis method (38). Restriction digests and ligations were carried out as recommended by the manufacturers (Amersham, Boehringer Mannheim, and Gibco BRL). Restriction fragments were isolated from agarose gels by using a Qiaquick gel extraction kit (Qiagen). The $CaCl_2$ method for preparing competent cells was routinely used (38).

Construction of plasmid pSH1 and generation of precise and random *fdo-blaM* fusions. To generate plasmid pSH1 (Fig. 1), plasmid pHA3, which encodes the entire *fdo* operon (1), was digested sequentially with *Hin*dIII and *Sac*I, and the resulting 5-kb fragment was ligated into similarly digested plasmid pYZ4, a Km^r derivative of the low-copy-number vector pBR322 (12). Four in-frame FdoG-BlaM fusions were created at precise restriction sites. pSH1 was digested with a mixture of either *Hin*cII plus *Eco*RI, *Hpa*I plus *Eco*RI, *Eco*RV plus *Eco*RI, or *Dra*I plus *Eco*RI; the longer fragment was purified and ligated with a *blaM* cassette, lacking both a promoter and a signal sequence, that was isolated from pYZ5 (12) by using *Pvu*II and *Eco*RI. To generate random *fdo-blaM* fusions, plasmid pSH1 was digested with *Asp718* and *Sac*I to produce exonuclease III-sensitive and -resistant sites, respectively. This plasmid DNA was treated with a Pharmacia nested deletion kit according to the manufacturer's instructions to create progressively truncated forms of the *fdo* locus. DNA samples from time points were purified, digested with *Eco*RI, and ligated with the *blaM* cassette (Fig. 1). All ligation mixtures were used to transform *E. coli* NM522. Transformed cells were plated on LB-kanamycin plates, and in-frame *fdoG′-*, *fdoH′-*, *fdoI′-blaM* fusions were isolated as described by Zhang and Broome-Smith (49) by patching colonies onto LB agar plates containing 20 μg of ampicillin/ml. Plasmid DNA from resistant clones was characterized by restriction endonuclease digestion with *Dra*I, *Bam*HI, and *Pvu*II.

Construction of *fdoG′-blaM-′fdoG* sandwich gene fusions. Three site-specific *fdoG′-blaM* sandwich fusions were created by using PCR-amplified DNA. A 2.3-kb *Hin*dIII-*Sma*I fragment encoding the N terminus of FdoG (647 amino acids) was ligated into similarly digested plasmid pUC19. Site-directed mutagenesis by overlap extension (20) was performed to introduce unique *Bam*HI restriction sites within *fdoG*, using one primer (5′-CAGCTATGACCATGATTACG-3′) located upstream of the *fdoG* promoter and individual primers BamSF1 (5′-CGATATGGAAGATGGATCCTTTGGCG-3′) for $FdoG_{74}$-BlaM, BamSF2 (5′-CCATTTATCGGATCCTGGCGCACGG-3′) for $FdoG_{118}$-BlaM, and BamSF3 (5′-CAGCGTCATGGATCCTGGCAG-3′) for $FdoG_{466}$-BlaM. PCR products were purified, cut with *Hin*dIII and *Bam*HI, and introduced into the corresponding cloning sites of the Cm^r plasmid pSU9 to generate pSB1, pSB2, and pSB3, respectively. In parallel, using one primer (5′-CACGACGTTGTAAAACGACG-3′) located downstream of the 2.3-kb *fdoG* insert and the three individual primers RevBamSF1, RevBamSF2, and RevBamSF3, which are the reverse complements of the three primers cited above, three independent PCR products were obtained, cut with *Bam*HI and *Sma*I, and ligated into similarly digested plasmids pSB1, pSB2, and pSB3 to generate unique *Bam*HI sites in *fdoG*. Then the 0.8-kb leaderless *blaM* gene fragment was excised from pCHAP4054 by digestion with *Bam*HI and inserted into the newly engineered restriction endonuclease sites. Finally the resulting plasmids pSF1, pSF2, and pSF3 were digested with *Hin*dIII and *Stu*I, and the fragments carrying the *fdoG′-blaM-′fdoG* sandwich fusions were introduced into the corresponding sites of pSH1 to generate pG74HI, pG118HI, and pG466HI.

Nucleotide sequencing of *fdo-blaM* fusion junctions. Plasmid DNA was denatured and sequenced with a T7 sequencing Kit (Pharmacia). The gene fusion point between the *fdoG*, *fdoH*, or *fdoI* gene and the truncated *blaM* gene was sequenced by using oligonucleotide BLA1 (5′-CTCGTGCACCCAACTGA-3′), which is complementary to the noncoding strand of the β-lactamase gene 40 bp from the fusion point. Each fusion point was sequenced on only one strand.

Ampicillin resistance of *E. coli* NM522 expressing Fdo–β-lactamase hybrid proteins. Bacteria were grown overnight in LB medium, and 4 μl of a 10^{-5} dilution was spotted on LB agar plates containing increasing amounts of ampicillin (0 to 500 μg/ml). Plates were incubated at 30°C aerobically for 16 h. To ensure reproducible results, the ampicillin plates were prepared freshly on the day of use, and data were collected from duplicates of at least three independent experiments. The MIC in micrograms of ampicillin per milliliter required to prevent colony formation by single cells was determined.

Switching of the *blaM* and *lacZ* reporter genes. To convert some of the isolated *fdoG′-blaM* fusions into *fdoG′-lacZ* fusions, we used in vitro recombinant DNA procedures. *Xmn*I restriction fragments from different *fdoG′-blaM* fusions were ligated into the *Sma*I-cut *lacZ* gene fusion vectors pNM481 and pNM482 (31). These constructions replace the originally present indicator gene *blaM* by *lacZ* without altering the fusion junction originally present in the *fdoG′-blaM* hybrid genes.

Enzyme assays. FDH-PMS activity was assayed spectrophotometrically at 30°C by monitoring the formate-dependent PMS-mediated reduction of 2,6-

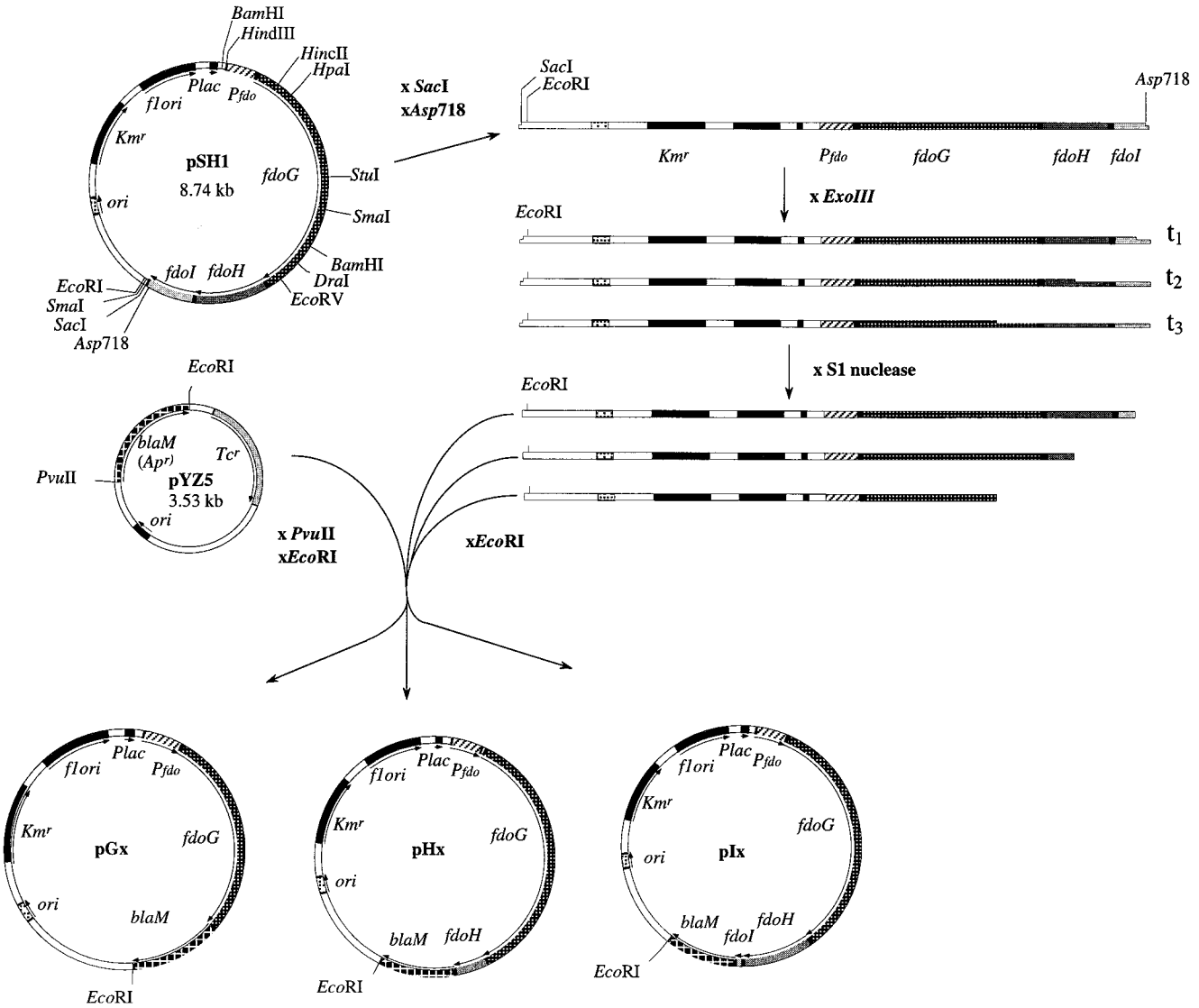

FIG. 1. Map of plasmid pSH1 and construction of random *fdo'-blaM* fusions. Plasmid pSH1 was made by ligation of the 5-kb *Hin*dIII-*Sac*I fragment from plasmid pHA3 (1) into the corresponding sites in vector pYZ4 (49). The cloned fragment carries the entire *fdo* locus with its own promoter. Random β-lactamase fusions were subsequently constructed by digesting from the 3′ end of the *fdoI* gene with exonuclease III and ligating the blunt-ended DNA with the truncated *blaM* gene.

dichlorophenolindolphenol as described previously (47). β-Galactosidase activity in chloroform-sodium dodecyl sulfate (SDS)-permeabilized cells was assayed as described by Miller (30).

Immunoblot analysis. Samples were prepared by boiling in Laemmli SDS sample buffer (24). Proteins were separated by SDS–12.5% polyacrylamide gel electrophoresis (SDS-PAGE) and electrotransferred onto a polyvinylidene difluoride membrane. Immunoblotting was performed by the Amersham enhanced chemiluminescence method according to the manufacturer's instructions. Antisera were used at the following dilutions: rabbit anti-β-lactamase polyclonal antiserum (5Prime → 3Prime, Inc.), 1/5,000; anti-hydrogenase 2 (HYD2), 1/15,000; and goat anti-rabbit immunoglobulin G-peroxidase, 1/10,000.

Spheroplasting and protease accessibility of FdoH–β-lactamase hybrid proteins. Spheroplasts were prepared from whole bacterial cells by a lysozyme-EDTA method (34), and the periplasmic fraction was separated from the spheroplasts by centrifugation at 13,000 rpm for 10 min. Pellets were resuspended in 200 μl of 100 mM Tris-HCl (pH 8), and 20 mM $MgSO_4$ was added to stabilize the spheroplasts. Aliquots of 50 μl were incubated for 30 min on ice with various amounts of proteinase K (Boehringer), and proteolysis was stopped by adding 5 μl of 100 mM phenylmethylsulfonyl fluoride. After a further 3 min, Laemmli SDS buffer was added and the samples were treated as described above.

Labelling of cells and protease mapping studies. Strain K38(pGP1-2) harboring pT7-6-derived plasmid pHA3 carrying the entire *fdo* locus (1) was grown anaerobically at 30°C in LB medium supplemented with 2 μM sodium selenite and ammonium molybdate and harvested in mid-log phase. The three FdoG, FdoH, and FdoI proteins were specifically expressed and labelled for 3 min with L-[^{35}S]methionine-cysteine (Promix; 10 μCi/μl; Amersham) after a shift to 42°C as described by Tabor and Richardson (41). Cells were then spun at 13,000 rpm in a benchtop centrifuge, washed, and resuspended either in Laemmli SDS buffer (crude extract) or in spheroplast buffer (34). Spheroplasts were incubated either with trypsin (2.5 mg/ml, 60 min at 37°C) or with proteinase K (300 μg/ml, 30 min on ice). One aliquot of spheroplasts was resuspended in water, subjected to three cycles of freezing-thawing, and incubated with proteinase K. After addition of trypsin soybean inhibitor (0.5 mg/ml) or phenylmethylsulfonyl fluoride (10 mM) to stop proteolysis, proteins were separated by SDS-PAGE and visualized by autoradiography. Immunoblotting with anti-HYD2 antiserum was performed with the same samples as a control for the spheroplasting experiment (37).

RESULTS

Construction of β-lactamase fusions to FdoG, FdoH, and FdoI. The hydropathy profile of the three subunits, α, β, and γ, of FDH-O was derived by the method of Kyte and Doolittle (23) with a window size of 11 residues (Fig. 2). The largest (113-kDa) FdoG polypeptide was predicted to possess an over-

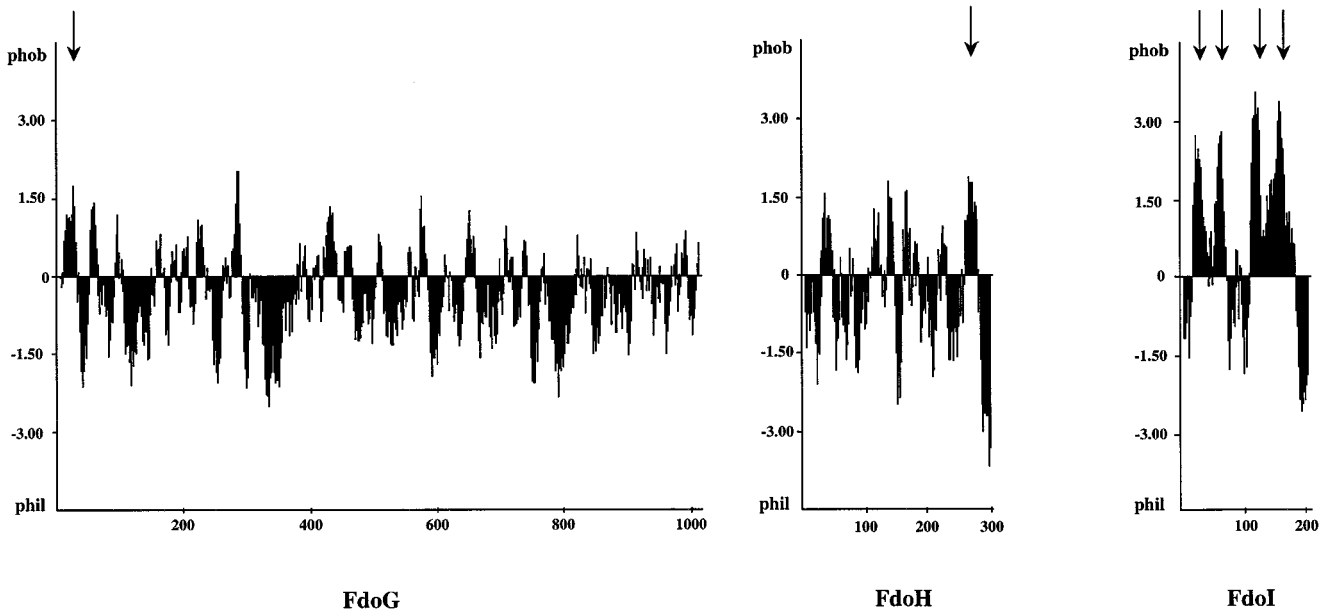

FIG. 2. Hydropathy analysis of the FdoG, FdoH, and FdoI subunits. The hydropathy plot was derived by using the algorithm of Kyte and Doolittle (23) with a window size of 11 residues. Arrows indicate putative transmembrane segments.

all highly hydrophilic content, with a hydrophobic N terminus possibly corresponding to a signal sequence. The 33-kDa FdoH polypeptide was suggested to be essentially hydrophilic, with a C-terminal membrane-spanning α helix extending from residues 260 to 280. The 25-kDa FdoI polypeptide was predicted to contain four stretches of hydrophobic residues with lengths of 19 to 21 amino acids alternating with hydrophilic or less hydrophobic portions of the polypeptide chain. This pattern is consistent with the role of the γ subunit as cytochrome *b*.

To determine the membrane topology of these three subunits more precisely, we constructed in-frame fusions between the *fdoG*, *fdoH*, and *fdoI* genes and the *blaM* reporter gene. Results for a representative set of 47 random fusions (Fig. 1), 4 site-specific fusions, and 3 sandwich fusions are given in Table 2. The position of the β-lactamase, i.e., cytoplasmic or periplasmic, was assessed on the basis of the MIC of ampicillin for the fusion proteins expressed from single cells. Fusions of BlaM to a cytoplasmic domain confer resistance to a low ampicillin concentration (3 to 25 μg/ml), whereas fusions to a periplasmic domain confer resistance to much higher levels of ampicillin (100 to 500 μg/ml) (Table 2). As the FDH-O complex is synthesized under either aerobic or anaerobic conditions (1), we investigated the influence of cell growth in the absence of oxygen on the sensitivity of isolated colonies to ampicillin. No difference was observed.

Synthesis of fusion proteins. To ensure that the levels of fusion protein expression were not affecting the topological analysis, we performed immunoblotting experiments with whole-cell extracts containing representative fusion proteins. Total proteins were separated by SDS-PAGE, and the hybrid proteins were then visualized with anti-β-lactamase serum (Fig. 3). As expected, sizes of hybrid proteins were compatible with the distribution of the fusion junctions along the *fdoG*, *fdoH*, and *fdoI* genes. A few hybrid proteins showed some degree of instability, yielding in particular degradation products that were often smaller than mature β-lactamase (Fig. 3A, lanes 6 and 7; Fig. 3B, lane 8; Fig. 3C, lane 8). Some fusion proteins (Arg_{36}FdoG-BlaM and Gly_{34}FdoI-BlaM) were particularly unstable since they were not detectable under these conditions (Fig. 3A, lane 8; Fig. 3C, lane 3). However, it should be noted that the hybrid protein Arg_{36}FdoG-BlaM was clearly visible after radiolabelling by using the T7 promoter-polymerase procedure (data not shown). There was no correlation between the stability of the different fusion proteins and the level of enzyme activity produced by the fusion proteins resulting from their cellular localization. For example, the unstable Gly_{34}FdoI-BlaM fusion protein displayed an MIC of 250 μg/ml, indicating a periplasmic localization, whereas the low-MIC Val_{155}FdoG-BlaM, Ala_{191}FdoI-BlaM, and Tyr_{199}FdoI-BlaM fusion proteins, compatible with a cytoplasmic localization, exhibited intense bands with good stability (Fig. 3A, lane 6; Fig. 3C, lanes 7 and 8). The lack of correlation between MICs and the amount of fusion expression was previously noticed in other topological analyses of membrane proteins using the same reporter protein (19, 42). We therefore concluded that the amount of fusion protein expressed did not affect the topological analysis.

Topological model of the FdoG protein. The low MICs for all FdoG-BlaM fusions tested, decreasing from 25 μg of ampicillin/ml in the N-terminal part to 4 μg of ampicillin/ml in the C-terminal part of the protein (Table 2) did not favor localization of the topological reporter in the periplasm but rather suggested that the overall FdoG subunit was exposed to the cytoplasm. It has been reported that a potential limitation of this gene fusion approach is posed by the finding that BlaM, when fused to particular cytoplasmic domains, occasionally displays an anomalous periplasmic phenotype due to the disruption of the integrity of the cytoplasmic membrane (12). Intermediate levels of ampicillin resistance (up to 25 μg/ml) observed with fusions at the amino-terminal end of FdoG might result from interaction of fusions with the membrane. It should be noted that use of β-lactamase sandwich fusions (Ser_{74}FdoG, Ser_{118}FdoG, and Gly_{466}FdoG) led to comparable results (Table 2). This observation confirmed that, when synthesized in physiological conditions in the presence of stoichi-

TABLE 2. Ampicillin resistance of *fdo-blaM* translational fusions

Subunit	Plasmid[a]	Fusion point[b]	Ampicillin concn (μg/ml) causing cell death	β-Lactamase location[c]
FdoG	pG36	Arg_{36}	25	C
	pG74HI	Ser_{74}	20	C
	pG86	Val_{86}	25	C
	pG118HI	Ser_{118}	4	C
	pG126	Trp_{126}	20	C
	pG155	Val_{155}	10	C
	pG218	Val_{218}	15	C
	pG228	Val_{228}	15	C
	pG239	Val_{239}	15	C
	pG244	Ala_{244}	15	C
	pG313	Arg_{313}	7.5	C
	pG317	Gly_{317}	7.5	C
	pG378	Asn_{378}	7.5	C
	pG406	Phe_{406}	7.5	C
	pG423	Arg_{423}	5	C
	pG458	Gly_{458}	4	C
	pG466HI	Gly_{466}	4	C
	pG489	Pro_{489}	4	C
	pG490	Leu_{490}	4	C
	pG698	Asn_{698}	4	C
	pG776	Arg_{776}	4	C
	pG876	Phe_{876}	4	C
	pG967	Asp_{967}	4	C
FdoH	pH40	Ile_{40}	3	C
	pH51	Glu_{51}	3	C
	pH61	Asn_{61}	2	C
	pH128	Phe_{128}	2	C
	pH136	Cys_{136}	2	C
	pH150	Leu_{150}	3	C
	pH168	Val_{168}	2	C
	pH205	Thr_{205}	2	C
	pH207	Gly_{207}	4	C
	pH264	Gly_{264}	2	C
	pH282	Asn_{282}	420	P
	pH290	Asn_{290}	500	P
	pH292	His_{292}	440	P
FdoI	pI2	Lys_{2}	2	C
	pI23	Phe_{23}	2	C
	pI31	Ser_{31}	100	P
	pI34	Gly_{34}	250	P
	pI36	Leu_{36}	120	P
	pI37	Phe_{37}	250	P
	pI105	Gly_{105}	5	C
	pI123	Val_{123}	100	P
	pI133	Trp_{133}	180	P
	pI137	Phe_{137}	100	P
	pI148	Phe_{148}	40	P
	pI150	Leu_{150}	100	P
	pI191	Ala_{191}	4	C
	pI192	Lys_{192}	4	C
	pI193	Lys_{193}	4	C
	pI196	Pro_{196}	2	C
	pI197	Arg_{197}	2	C
	pI199	Tyr_{199}	3	C

[a] Most were made by exonuclease III deletions of pSH1. Sandwich fusion plasmids pG74HI, pG118HI, and pG466HI were created at unique *Bam*HI restriction sites, using PCR site-directed mutagenesis. Plasmids pG86, pG155, pG876, and pG967 were constructed at precise *Hin*cII, *Hpa*I, *Dra*I, and *Eco*RV restriction sites of the *fdoG* gene, respectively.

[b] Last amino acid residue of the Fdo subunit before the fusion point.

[c] P, Periplasmic; C, cytoplasmic.

ometric amounts of the β and γ subunits, the α subunit is likely to be located in the cytoplasm.

Additional experiments were carried out to test this model. First, the *blaM* indicator gene was exchanged with the *lacZ* gene to convert some of the originally isolated *fdoG*::*blaM* fusions to *fdoG*::*lacZ* fusions. Since LacZ is active only in the cytoplasmic fraction, an opposite pattern of enzyme activity would be expected for the FdoG-LacZ hybrid proteins. Despite repeated attempts, we were not able to construct in vitro stable β-galactosidase fusions at residues Val_{86}, Trp_{126}, Val_{155}, Phe_{406}, and Arg_{423}, located in the N-terminal part of the FdoG subunit. This difficulty could be accounted for at least by the partial embedding of the enzyme within the membrane, preventing proper folding or tetramerization and enzymatic activity (14). Similarly, partial insertion of the β-lactamase moiety in the cytoplasmic membrane in the case of N-terminal FdoG fusions (from residues Arg_{36} to Phe_{406}) would explain why MICs were higher than those reported for the C-terminal fusions of FdoG (Table 2). In contrast, cells harboring the in vitro-converted fusion Gly_{458}FdoG-LacZ were isolated as red colonies on MacConkey lactose indicator plates. They exhibited a significant β-galactosidase specific activity of 200 Miller units per ml of culture (30), which corroborated the expected location of this fusion in the cytoplasm as deduced from the originally isolated Gly_{458}FdoG-BlaM fusion (Table 2).

Topological model of the FdoH subunit. β-Lactamase fusions to the FdoH subunit extending from the N terminus of the protein (at residue Ile_{40}) to the very beginning of the predicted membrane-spanning segment (at residue Gly_{264}) confer sensitivity to very low concentrations of ampicillin (2 to 4 μg/ml) (Table 2), suggesting a cytoplasmic localization for the β-lactamase moiety. Following the transmembrane segment predicted from residues 260 to 280, three fusions enabling the cells to grow on high ampicillin concentrations (420 to 500 μg/ml) were obtained at amino acids Asn_{282}, Asn_{290}, and His_{292}. This observation was in favor of a periplasmic location for the C terminus of FdoH. The combined results from the FdoH hydropathy profile (Fig. 2) and from the MICs for the FdoH-BlaM fusion proteins suggest a topological arrangement of FdoH such that the majority of the polypeptide including the N terminus is in the cytoplasm and the C terminus is in the periplasm (Fig. 4A).

To confirm this model, proteinase K susceptibility of FdoH-BlaM hybrid proteins was analyzed in cells converted to spheroplasts. Fusions at residues Thr_{205} and Asn_{290} were chosen as target proteins because they were supposed to be located on each side of the cytoplasmic membrane. Detection of these proteins was performed by Western blotting. The Thr_{205}FdoH-BlaM fusion protein was found to be highly resistant to proteolysis (Fig. 4B, lanes 1 to 4), whereas the Asn_{290}FdoH-BlaM hybrid protein was shown to be progressively digested by increasing concentrations of proteinase K (Fig. 4B, lanes 5 to 8). Thus, as expected from the model proposed in Fig. 4A, fusion Thr_{205} was protected by an intact cytoplasmic membrane and fusion Asn_{290} at the C terminus was exposed to the periplasm.

Topological model of the FdoI subunit. The pattern of resistance to ampicillin of the fusions (Table 2) was compatible with a four-transmembrane-span model of FdoI as predicted from the hydropathy profile (Fig. 2). The range of MICs between cytoplasmically and periplasmically located fusions varied from 10- to 100-fold. Fusions at the N and C termini all exhibited very low levels of resistance to ampicillin, indicating that both extremities of FdoI have a cytoplasmic location. The unique fusion at residue Gly_{105} isolated in the second loop region situated between the second and the third transmembrane segments also displayed a weak MIC, in agreement with a cytoplasmic exposition. These observations corroborate the distribution of the transmembrane segments as depicted in Fig. 5. According to the positive-inside rule applying to bacterial

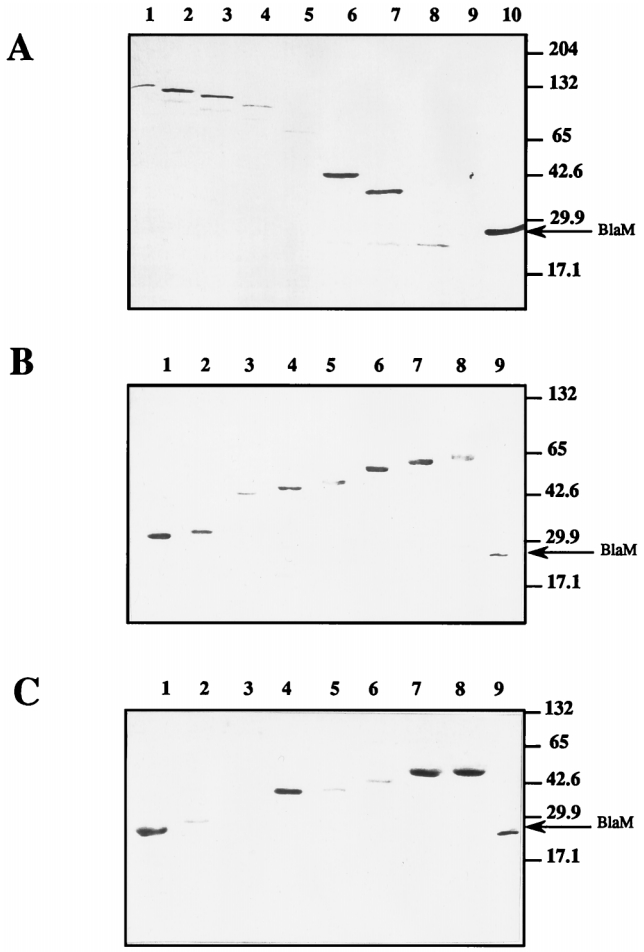

FIG. 3. Western blots of FdoG-BlaM, FdoH-BlaM, and FdoI-BlaM fusion proteins. Equal amounts of cell extracts were electrophoresed on SDS–12.5% polyacrylamide gels, and β-lactamase fusion proteins were visualized by immunoblotting with polyclonal antibodies against BlaM. (A) Cell extracts of strain NM522 containing *fdoG′-blaM* fusion plasmids. Amino acids at which fusions occur: lane 1, Asp_{967}; lane 2, Phe_{876}; lane 3, Arg_{776}; lane 4, Asn_{698}; lane 5, Arg_{423}; lane 6, Val_{155}; lane 7, Val_{86}; lane 8, Arg_{36}; lane 9, none (parental NM522). Lane 10, TEM β-lactamase from pBR322 (29 kDa). (B) Cell extracts of NM522 containing *fdoH′-blaM* fusion plasmids. Lane 1, Ile_{40}; lane 2, Asn_{61}; lane 3, Cys_{136}; lane 4, Val_{168}; lane 5, Thr_{205}; lane 6, Gly_{264}; lane 7, Asn_{282}; lane 8, Asn_{290}; lane 9, TEM β-lactamase from pBR322. (C) Cell extracts of NM522 containing *fdoI′-blaM* fusion plasmids. Lane 1, Lys_2; lane 2, Phe_{23}; lane 3, Gly_{34}; lane 4, Gly_{105}; lane 5, Val_{123}; lane 6, Leu_{150}; lane 7, Ala_{191}; lane 8, Tyr_{199}; lane 9, TEM β-lactamase from pBR322.

inner membrane proteins (44), the positively charged residues Arg and Lys are four times more prevalent in cytoplasmic connecting segments than in periplasmic loops. In agreement with this observation, we found a total of 21 positive charges in the cytoplasmic loops of FdoI but only 3 in the periplasmic loops.

Protease accessibility of FDH-O in spheroplasts. To confirm the topological model of FDH-O, we investigated protease sensitivity of the three subunits in spheroplasts. K38 cells carrying plasmids pGP1-2 and pHA3, which expresses the wild-type FDH-O protein complex, were grown anaerobically, labelled with [^{35}S]cysteine-methionine in the presence of rifampin, and converted to spheroplasts. A sample of the spheroplasts was lysed with several cycles of freezing-thawing. Untreated and treated spheroplasts were incubated with or without proteinase K or trypsin, and the resulting labelled polypeptides were analyzed by SDS-PAGE (Fig. 6A). In addition to the three FDH-O subunits, α (113 kDa), β (33 kDa), and γ (25 kDa), visualized in spheroplasts and cell extracts (Fig. 6A, lanes 1, 2, and 9), a nonspecific band of about 20 kDa was detected. This band was digested by trypsin or proteinase K (Fig. 6A, lanes 3, 5, and 7). The three FDH-O subunits were protected from trypsin as well as proteinase K digestion in intact spheroplasts (Fig. 6A, lanes 3 and 5). In contrast, α and β subunits were completely degraded by proteinase K when the spheroplasts were lysed, and only a reduced amount of the γ subunit remained visible (Fig. 6A, lane 7). The observed pattern of sensitivity is thus consistent with a cytoplasmic location for α and β and a transmembrane location for γ, which could account for a significant resistance of this subunit to proteolysis. To assess the efficiency of spheroplast formation and of protease accessibility, the pattern of *E. coli* membrane-bound HYD2 was monitored by immunoblotting with antibodies against HYD2 (Fig. 6B). HYD2, which consists at least of one large (61-kDa) and one small (30-kDa) subunit, has been shown to be released from the membrane by trypsin treatment (3) and to be attached to the periplasmic side of the cytoplasmic membrane after translocation (37). As expected from previous data, the small subunit was accessible to both proteases and cleaved as a 25-kDa product from spheroplasts (Fig. 6B, lanes 3, 5, and 7), whereas the large subunit was recovered in the trypsin- or proteinase K-solubilized fractions (Fig. 6B, lanes 4, 6, and 8). As a consequence, the interpretation of the digestion data is consistent with the model proposed from the fusions.

FDH-PMS activity of the β-lactamase fusion proteins. The Km^r Tc^r *fdo-fnr* mutant HA55, which is defective in both FDH-N and FDH-O activities (1), was first used as a recipient strain to test the ability of plasmid-borne β-lactamase fusions to display FDH-PMS activity. As a control, plasmid pHA3, carrying the entire *fdoGHI* locus, was shown to confer a specific activity of 0.2 μmol of formate oxidized per mg (dry weight) of bacteria per min. Plasmids pG36, pH292, and pI150, carrying representative β-lactamase fusions in each of the three subunits, were chosen because they harbored a sufficiently high level of ampicillin resistance (Table 2) to be selected by directly plating the transformed cells on ampicillin plates. No FDH-PMS activity was detected. The MC4100-*fnr* Tc^r strain, deficient in FDH-N activity, was subsequently transformed with another set of plasmid β-lactamase fusions expressing a low resistance to ampicillin. Selected Km^r transformants harboring plasmid pG458, pG967, pH205, or pI105 displayed the same low level of FDH-PMS activity (0.04 μmol of formate oxidized per mg [dry weight] of bacteria per min) as the recipient strain, which originated from the chromosomal copy of the *fdoGHI* locus. However, when plasmid pI196 was introduced into MC4100-*fnr*, a significant threefold increase in FDH-PMS activity (0.14 μmol of formate oxidized per mg of bacteria per min) was measured. These results suggest that the three α, β, and (nearly entire) γ subunits are required for recovery of FDH-PMS activity.

DISCUSSION

Arrangement of the electron transfer and catalytic subunits of complex redox proteins in the bacterial cytoplasmic membrane is directly associated with the generation of energy via a proton electrochemical gradient resulting from translocation of protons across the membrane. Classically, redox loop models have been proposed as responsible for this energy conservation by the net transfer of negatively charged electrons from the periplasm to the cytoplasm, whereas protons are released

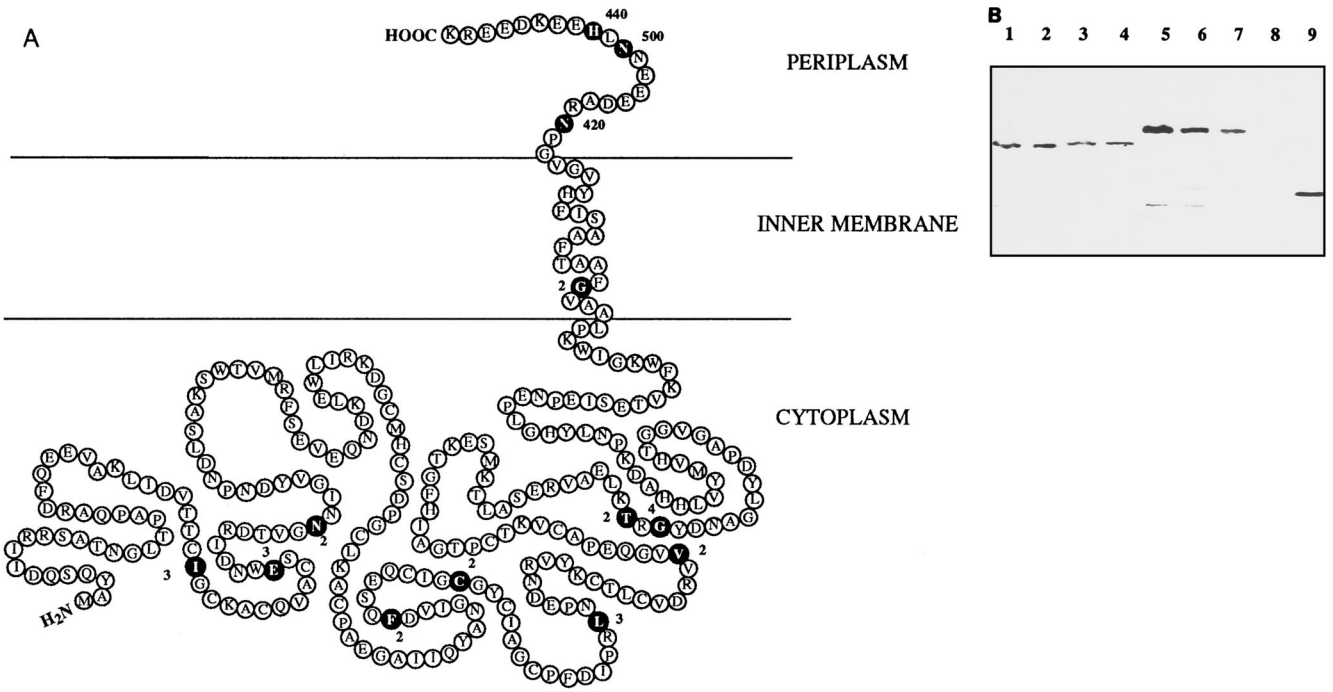

FIG. 4. Model for the topological organization of FdoH and protease susceptibility of FdoH-BlaM hybrid proteins in spheroplasts. (A) Model based on the properties of the FdoH–β-lactamase fusions and the hydropathy plot. Fusions are indicated by black circles, and the adjacent numbers correspond to MICs in micrograms of ampicillin per milliliter. (B) Visualization by Western blotting of the sensitivity of two FdoH-BlaM fusion proteins to proteinase K digestion in spheroplasts. Lanes 1 to 4, strain NM522 carrying the plasmid-encoded Thr_{205}FdoH-BlaM gene fusion; lanes 5 to 8, strain NM522 carrying the plasmid-encoded Asn_{290}FdoH-BlaM gene fusion; lane 9, strain NM522(pBR322) expressing wild-type TEM β-lactamase. Proteinase K was added at a final concentration of 0 (lanes 1 and 5), 200 (lanes 2 and 6), 500 (lanes 3 and 7), or 1,000 (lanes 4 and 8) μg/ml.

in the periplasmic compartment (32). The membrane-bound respiratory nitrate reductase which is induced under anaerobic growth conditions in the presence of nitrate provides the best-characterized example of this kind of redox loop in the enterobacterium *E. coli* (15). This enzymatic complex catalyzes electron transfer from quinol to nitrate coupled to proton release in the periplasm, compatible with a mechanism of energy conservation (22). It is composed of a two-subunit catalytic and electron transfer domain facing the cytoplasm and anchored to the membrane by a five-hydrophobic-transmembrane-span *b*-type cytochrome subunit. Such a topology is supported by biochemical and biophysical evidence (2, 26, 27). In contrast, relatively little is known about the subcellular organization of the two formate dehydrogenase isoenzymes, FDH-N and FDH-O, which can be coupled to the reduction of nitrate when formate is supplied as the electron donor (1, 36). Based on

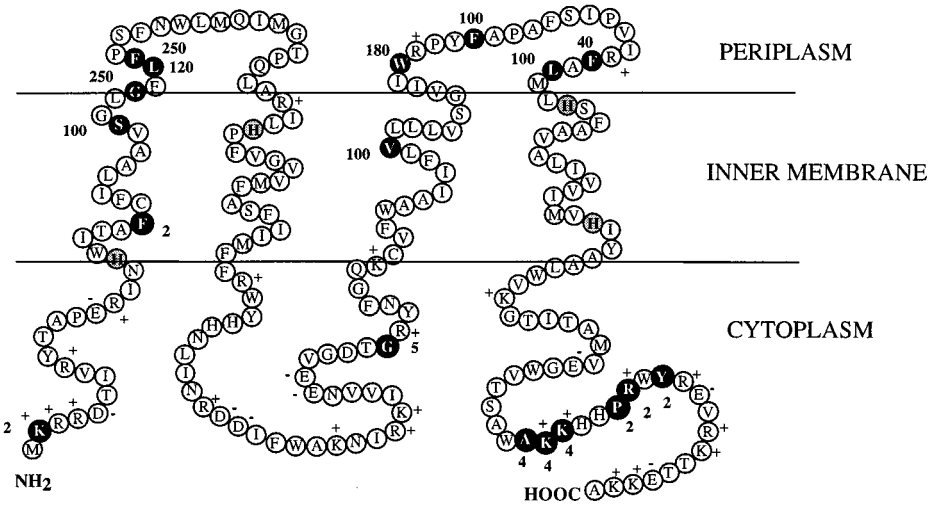

FIG. 5. Model for the topological organization of FdoI, based on the properties of β-lactamase fusions, the hydropathy plot, and the positive-inside rule (44). β-Lactamase fusions are indicated by black circles, and the adjacent numbers correspond to MICs in micrograms of ampicillin per milliliter. Conserved histidine residues that are proposed to act as heme iron ligands are indicated by shaded circles (8). The positions of positively and negatively charged residues are shown.

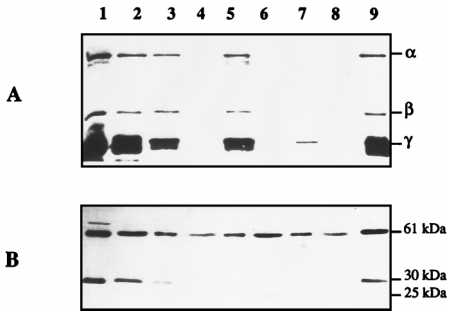

FIG. 6. Protease susceptibility of the ^{35}S-labelled *fdo* gene products. (A) Proteins were labelled with L-[^{35}S]methionine-cysteine in K38 harboring pGP1-2 after induction at 42°C and addition of rifampin by the method of Tabor and Richardson (41). Cells were converted to spheroplasts and incubated with or without proteinase K or trypsin. Lane 1, untreated cell extracts; lane 2, untreated spheroplasts; lane 3, spheroplasts with 2.5 mg of trypsin/ml; lane 4, trypsin-solubilized fraction; lane 5, spheroplasts with 300 μg of proteinase K/ml; lane 6, proteinase K-solubilized fraction; lane 7, lysed spheroplasts with 300 μg of proteinase K/ml; lane 8, proteinase K-solubilized fraction (lysed spheroplasts); lane 9, lysed spheroplasts. (B) The same samples were subjected to Western blotting using anti-HYD2 antibodies. The three subunits, α, β, and γ, of FDH-O, as well as the large subunit (61 kDa), the small subunit (30 kDa), and the trypsin-released small-subunit derivative (25 kDa) of HYD2 are indicated on the right.

nucleotide sequencing data and the presence of a two-arginine leader, the large subunit of FDH-N was suggested to be located at the periplasmic surface (6, 7). However, no evidence for such a location has been gained so far from experimental data.

In this study, we investigated the membrane topology of the whole FDH-O heterotrimeric enzyme by use of the genetic *blaM* gene fusion approach, whose utility has been proven for analyzing the membrane assembly of a number of bacterial proteins (12), including the anchor subunit of the *E. coli* terminal electron transfer DMSO reductase (46). These results combined with examination of proteolytic susceptibility of the complex allowed us to propose a topological model which differs appreciably from the previously suggested location for the two respiratory FDH isoenzymes mainly inferred from sequence data (6, 8, 40). In addition, both the α and β subunits of the major anaerobic respiratory FDH-N enzyme had previously been reported to occupy a transmembranous location within the cytoplasmic membrane, based on analysis of the organization of the enzyme by direct covalent modification with non-membrane-permeant reagents (18). However, this arrangement is not consistent with knowledge drawn from the recent resolution of the structure of the fermentative FDH (FDH-H) (11), discussed below. In our model, the two FdoG and FdoH subunits, which contain the catalytic site for formate oxidation and the electron transfer polypeptide, respectively, appear to be located on the cytoplasmic side of the membrane. First, the MICs for the *blaM* fusions were low in both cases, except for the C-terminal part of FdoH, whose last 20 amino acids protrude into the periplasm and can serve as a membrane anchor for the αβ catalytic domain. Second, protease susceptibility experiments revealed that both FdoG and FdoH are protected in spheroplasts but accessible to proteolytic degradation after lysis of spheroplasts, which implies a cytoplasmic location. In perfect agreement with the predictions derived from von Heijne's positive-inside rule (44), in which cytoplasmic domains of membrane proteins are enriched in lysine and arginine residues, the FdoI subunit specifying cytochrome *b* is demonstrated to contain four transmembrane segments with both the N and C termini in the cytoplasm.

It has been reported that the processes of export of small and large subunits of hydrogenases are codependent and that the absence of one subunit blocks the processing and export of the partner subunit (29, 37, 43). To exclude a possible equivalent effect of the absence of FDH-O β and γ subunits on the correct location of the α subunit, we constructed three FdoG–β-lactamase sandwich fusions allowing the simultaneous expression of FdoH and FdoI in stoichiometric amounts. The same low MICs were reported, in agreement with a location of FdoG in the cytoplasm.

Like a large number of proteins which are associated with redox cofactors, the FdoG protein possesses the N-terminal RRXFXK motif, which is thought to serve as the targeting sequence for the Sec-independent translocation to the periplasm (7). By fusing the NiFe hydrogenase small subunit signal peptide from *Desulfovibrio vulgaris* to the leaderless β-lactamase of *E. coli*, Nivière and coworkers were able to demonstrate that this sequence plays a specific role in the export mechanism of the fusion protein (33). No other experimental data concerning similar fusions with the β-lactamase reporter gene are available. Using the same technique, however, we did not observe any translocation of the various β-lactamase hybrid proteins constructed by fusion with the N-terminal two-arginine leader peptide from the FdoG subunit of the aerobic FDH (data not shown). It should be noted that care was taken to create a fusion, Arg_{36}FdoG-BlaM, very close to the putative cleavage site of the leader peptide, predicted at residue Ala_{33} by computer programs. Remarkably, a similar observation was recently made in a study using β-lactamase fusions with the N terminus of the catalytic DmsA subunit of DMSO reductase, which also contains the double-arginine signal sequence and is located in the cytoplasm (44a).

These results suggest that the positively charged double-arginine signal peptide is not by itself responsible for protein export. We propose that it could be involved in targeting FdoG to the membrane. An indication for this role is given by the ampicillin MICs (from 25 to 7.5 μg/ml) for the FdoG-BlaM fusions selected near the N terminus of FdoG, which are higher than MICs for the bona fide cytoplasmic fusions (4 to 5 μg/ml) but are too low (compared with MICs for periplasmic FdoH C terminus and FdoI segments) to indicate localization in the periplasm. These fusions exhibiting partial resistance to ampicillin could be considered to have the β-lactamase moiety bound to the cytoplasmic membrane and partly exposed to the periplasm.

The crystal structure of the fermentative isoenzyme FDH-H, belonging to the anaerobic formate hydrogen lyase complex, has been recently solved (11). FDH-H was shown to contain selenocysteine, molybdenum, two molybdopterin guanine dinucleotide cofactors, and an Fe_4S_4 cluster at the active site responsible for the oxidation of formate to carbon dioxide. More than 20 residues involved in the coordination of the two molybdopterin guanine dinucleotide cofactors and distributed along the entire FDH-H sequence are well conserved among the other two respiratory FDH catalytic subunits. Such a structural organization precludes the existence of FdoG protein segments on both sides of the membrane and thus favors a position for FdoG only on one side of the membrane.

Based on the striking similarity between the FDH-O and FDH-N isoenzymes (6, 35), we can speculate that the α and β subunits of FDH-N are likely exposed on the inner side of the cytoplasmic membrane. If this is the case, oxidation of intracellular formate could be directly catalyzed by either of the two FDH isoenzymes, depending on the environmental physiological conditions, thus preventing acidification of the cytoplasm. In this context, export of formate through the specific bidirec-

tional formate channel FocA (40) will not be required to provide the substrate for both enzymes. Demonstration that formate is oxidized at the inner surface of the membrane has been achieved by measurement of the electrochemical proton gradient generated by nitrate respiration in *E. coli* membrane vesicles (10). Further support for this contention was offered by measurement of $H^+/2e^-$ stoichiometries for formate oxidation catalyzed by the *E. coli* FDH (22). The topological model proposed here is fully consistent with these observations.

Among the cofactor-containing redox proteins having an RRXFXK two-arginine leader motif, the molybdoprotein DMSO reductase DmsABC of *E. coli* represents a notable exception since it has been established by experimental evidence to be located on the cytoplasmic surface of the membrane. Weiner et al. recently identified a Sec-independent translocation system encoded by a three-cistron operon, *mttABC*, which mediates membrane targeting and translocation of multimeric membrane-bound and periplasmic redox enzymes, including DmsABC (45). Our present study indicates that the three subunits of the FDH-O enzyme complex and DMSO reductase are similar in architecture, with an extrinsic catalytic and electron transfer dimeric domain bound to an intrinsic anchor subunit, which is a *b*-type cytochrome in the case of FDH-O. It is thus tempting to speculate that FDH-O assembled in a similar manner, and it would be of interest to examine the effect of the D-43 mutation in the *mttA* gene, which prevents the assembly of DmsAB on the membrane (45), on the cellular location and activity of FDH-O.

ACKNOWLEDGMENTS

We are grateful to D. H. Boxer for the gift of anti-HYD2 serum, T. Pugsley's group for providing plasmid pCHAP4054, and J. K. Broome-Smith for plasmids pYZ4 and pYZ5. We thank J. Robert-Baudouy for support and interest in this work and the members of the Laboratoire de Génétique Moléculaire des Microorganismes et des Interactions Cellulaires for helpful discussions and constant encouragement.

This work was supported by grants from the Centre National de la Recherche Scientifique and the Direction de la Recherche et des Etudes Doctorales to UMR 5577.

REFERENCES

1. **Abaibou, H., J. Pommier, S. Benoit, G. Giordano, and M. A. Mandrand-Berthelot.** 1995. Expression and characterization of the *Escherichia coli fdo* locus and a possible physiological role for aerobic formate dehydrogenase. J. Bacteriol. **177:**7141–7149.
2. **Augier, V. B., M. Guigliarelli, P. Asso, C. Bertrand, G. Frixon, G. Giordano, M. Chippaux, and F. Blasco.** 1993. Site-directed mutagenesis of conserved cysteine residues within the β subunit of *Escherichia coli* nitrate reductase. Physiological, biochemical, and EPR characterization of the mutated enzymes. Biochemistry **32:**2013–2023.
3. **Ballantine, S. P., and D. H. Boxer.** 1986. Isolation and characterisation of a soluble active fragment of hydrogenase isoenzyme 2 from the membranes of anaerobically grown *Escherichia coli*. Eur. J. Biochem. **156:**277–284.
4. **Bartolomé, B., Y. Jubete, E. Martinez, and F. de la Cruz.** 1991. Construction and properties of a family of pACYC184-derived cloning vectors compatible with pBR322 and its derivatives. Gene **102:**75–78.
5. **Begg, Y. A., J. N. Whyte, and B. A. Haddock.** 1977. The identification of mutants of *Escherichia coli* deficient in formate dehydrogenase and nitrate reductase activities using dye indicators plates. FEMS Microbiol. Lett. **2:**47–50.
6. **Berg, B. L., J. Li, J. Heider, and V. Stewart.** 1991. Nitrate-inducible formate dehydrogenase in *E. coli* K-12. I. Nucleotide sequence of the *fdnGHI* operon and evidence that opal (UGA) encodes selenocysteine. J. Biol. Chem. **266:** 22380–22385.
7. **Berks, B. C.** 1996. A common export pathway for proteins binding complex redox cofactors? Mol. Microbiol. **22:**393–404.
8. **Berks, B. C., M. D. Page, D. J. Richardson, A. Reilly, A. Cavill, F. Outen, and S. J. Ferguson.** 1995. Sequence analysis of subunits of the membrane-bound nitrate reductase from a denitrifying bacterium: the integral membrane subunit provides a prototype for the dihaem electron-carrying arm of a redox loop. Mol. Microbiol. **15:**319–331.
9. **Bolivar, F., R. L. Rodriguez, P. J. Greene, M. C. Betlach, H. L. Heynecker, H. W. Boyer, J. H. Crosa, and S. Falkow.** 1977. Construction and characterization of new cloning vehicles. II. A multipurpose cloning system. Gene **2:**95–113.
10. **Boonstra, J., and W. N. Konings.** 1977. Generation of an electrochemical proton gradient by nitrate respiration in membrane vesicles from anaerobically grown *Escherichia coli*. Eur. J. Biochem. **78:**361–368.
11. **Boyington, J. C., V. N. Gladyshev, S. V. Khangulov, T. C. Stadtman, and P. D. Sun.** 1997. Crystal structure of formate dehydrogenase H: catalysis involving Mo, molybdopterin, selenocysteine, and an Fe_4S_4 cluster. Science **275:**1305–1307.
12. **Broome-Smith, J. K., M. Tadayyon, and Y. Zhang.** 1990. β-Lactamase as a probe of membrane protein assembly and protein export. Mol. Microbiol. **4:**1637–1644.
13. **Enoch, H. G., and R. L. Lester.** 1975. The purification and properties of formate dehydrogenase and nitrate reductase from *Escherichia coli*. J. Biol. Chem. **250:**6693–6705.
14. **Froshauer, S., G. N. Green, D. Boyd, K. McGovern, and J. Beckwith.** 1988. Genetic analysis of the membrane insertion and topology of MalF, a cytoplasmic membrane protein of *Escherichia coli*. J. Mol. Biol. **200:**501–511.
15. **Gennis, R. B., and V. Stewart.** 1996. Respiration, p. 217–261. *In* F. C. Neidhardt, R. Curtis III, J. L. Ingraham, E. C. C. Lin, K. B. Low, B. Magasanik, W. S. Reznikoff, M. Riley, M. Schaechter, and H. E. Umbarger (ed.), *Escherichia coli* and *Salmonella*: cellular and molecular biology, 2nd ed. American Society for Microbiology, Washington, D.C.
16. **Giordano, R., C. L. Medani, M. A. Mandrand-Berthelot, and D. H. Boxer.** 1983. Formate dehydrogenases from *E. coli*. FEMS Microbiol. Lett. **17:**171–177.
17. **Gough, J. A., and N. E. Murray.** 1983. Sequence diversity among related genes for recognition of specific targets in DNA molecules. J. Mol. Biol. **166:**1–19.
18. **Graham, A., and D. H. Boxer.** 1981. The organization of formate dehydrogenase in the cytoplasmic membrane of *Escherichia coli*. Biochem. J. **195:** 627–637.
19. **Gunn, F. J., C. G. Tate, C. E. Sansom, and P. J. F. Henderson.** 1995. Topological analyses of the L-fucose-H+ symport protein, FucP, from *Escherichia coli*. Mol. Microbiol. **15:**771–783.
20. **Ho, S. N., H. D. Hunt, R. M. Morton, S. K. Pullen, and L. R. Pease.** 1989. Site directed mutagenesis by overlap extension using the polymerase chain reaction. Gene **77:**51–59.
21. **Iobbi-Nivol, C., C. L. Santini, F. Blasco, and G. Giordano.** 1990. Purification and further characterization of the second nitrate reductase of *Escherichia coli* K-12. Eur. J. Biochem. **188:**679–687.
22. **Jones, R. W.** 1980. Proton translocation by the membrane-bound formate dehydrogenase of *Escherichia coli*. FEBS Microbiol. Lett. **8:**167–171.
23. **Kyte, J., and R. F. Doolittle.** 1982. A simple method for displaying the hydropathic character of a protein. J. Mol. Biol. **157:**105–132.
24. **Laemmli, U. K.** 1970. Cleavage of structural proteins during the assembly of the head of bacteriophage T4. Nature (London) **227:**680–685.
25. **Lyons, L. B., and N. D. Zinder.** 1972. The genetic map of the filamentous bacteriophage f1. Virology **49:**45–60.
26. **MacGregor, C. H.** 1976. Biosynthesis of membrane-bound nitrate reductase in *Escherichia coli*: evidence for a soluble precursor. J. Bacteriol. **126:**122–131.
27. **Magalon, A., D. Lemesle-Meunier, R. A. Rothery, C. Frixon, J. H. Weiner, and F. Blasco.** 1997. Heme axial ligation by the highly conserved His residues in helix II of cytochrome *b* (NarI) of *Escherichia coli* nitrate reductase A (NarGHI). J. Biol. Chem. **272:**25652–25658.
28. **Manoil, C., J. J. Mekalanos, and J. Beckwith.** 1985. Tn*phoA*: a transposon probe for protein export signals. Proc. Natl. Acad. Sci. USA **82:**8129–8133.
29. **Menon, N. K., J. Robbins, J. C. Wendt, K. T. Shanmugam, and A. E. Przybyla.** 1991. Mutational analysis and characterization of the *Escherichia coli hya* operon, which encodes (NiFe) hydrogenase 1. J. Bacteriol. **173:**4851–4861.
30. **Miller, J. H.** 1992. A short course in bacterial genetics: a laboratory manual and handbook for *Escherichia coli* and related bacteria, p. 275–278. Cold Spring Harbor Laboratory Press, Cold Spring Harbor, N.Y.
31. **Minton, N. P.** 1984. Improved plasmid vectors for the isolation of translational *lac* gene fusions. Gene **31:**269–273.
32. **Mitchell, P.** 1979. Compartmentation and communication in living systems. Ligand conduction: a general catalytic principle in chemical, osmotic and chemiosmotic reaction systems. Eur. J. Biochem. **95:**1–20.
33. **Nivière, V., S. L. Wong, and G. Voordouw.** 1992. Site-directed mutagenesis of the hydrogenase signal peptide consensus box prevents export of a β-lactamase fusion protein. J. Gen. Microbiol. **138:**2173–2183.
34. **Osborn, M. J., J. E. Gander, E. Parisi, and J. Carson.** 1972. Mechanism of assembly of the outer membrane of *Salmonella typhimurium*. J. Biol. Chem. **247:**3962–3972.
35. **Plunkett, G., V. Burland, D. L. Daiels, and F. R. Blattner.** 1993. Analysis of the *Escherichia coli* genome. III. DNA sequence of the region from 87.2 to 89.2 minutes. Nucleic Acids Res. **21:**3391–3398.
36. **Pommier, J., M. A. Mandrand-Berthelot, S. E. Holt, D. H. Boxer, and G. Giordano.** 1992. A second phenazine methosulphate-linked formate dehy-

drogenase isoenzyme in *Escherichia coli*. Biochim. Biophys. Acta **1107:**305–313.
37. **Rodrigue, A., D. H. Boxer, M. A. Mandrand-Berthelot, and L. F. Wu.** 1996. Requirement for nickel of the transmembrane translocation of NiFe-hydrogenase 2 in *Escherichia coli*. FEBS Lett. **392:**81–86.
38. **Sambrook, J., E. F. Fritsch, and T. Maniatis.** 1989. Molecular cloning: a laboratory manual, 2nd ed. Cold Spring Harbor Laboratory Press, Cold Spring Harbor, N.Y.
39. **Silhavy, T. J., and J. R. Beckwith.** 1985. Use of *lac* fusions for the study of biological problems. Microbiol. Rev. **49:**398–418.
40. **Suppmann, B., and G. Sawers.** 1994. Isolation and characterization of hypophosphite-resistant mutants of *E. coli*: identification of the FocA protein, encoded by the *pfl* operon, as a putative formate transporter. Mol. Microbiol. **11:**965–982.
41. **Tabor, S., and C. C. Richardson.** 1985. A bacteriophage T7 RNA polymerase/promoter system for controlled exclusive expression of specific genes. Proc. Natl. Acad. Sci. USA **76:**4350–4354.
42. **Tate, C. G., and P. J. F. Henderson.** 1993. Membrane topology of the L-rhamnose-H+ transport protein (RhaT) from *Enterobacteria*. J. Biol. Chem. **268:**26850–26857.
43. **van Dongen, W., W. Hagen, W. van den Berg, and C. Veeger.** 1988. Evidence for an unusual mechanism of membrane translocation of the periplasmic hydrogenase of *Desulfovibrio vulgaris* (Hildenborough), as derived from expression in *Escherichia coli*. FEMS Microbiol. Lett. **50:**5–9.
44. **von Heijne, G.** 1986. The distribution of positively charged residues in bacterial inner membrane correlates with the trans-membrane topology. EMBO J. **5:**3021–3027.
44a. **Weiner, J. H.** Personal communication.
45. **Weiner, J. H., P. T. Bilous, G. M. Shaw, S. P. Lubitz, L. Frost, G. H. Thomas, J. A. Cole, and R. J. Turner.** 1998. A novel and ubiquitous system for membrane targeting and secretion of cofactor-containing proteins. Cell **93:**93–101.
46. **Weiner, J. H., G. Shaw, R. J. Turner, and C. A. Trieber.** 1993. The topology of the anchor subunit of dimethyl sulfoxide reductase of *Escherichia coli*. J. Biol. Chem. **268:**3238–3244.
47. **Wu, L. F., and M. A. Mandrand-Berthelot.** 1986. Genetic and physiological characterization of new *Escherichia coli* mutants impaired in hydrogenase activity. Biochimie **68:**167–179.
48. **Yanisch-Perron, C., J. Vieira, and J. Messing.** 1985. Improved M13 phage cloning vectors and host strains: nucleotide sequences of the M13mp18 and pUC19 vectors. Gene **33:**103–119.
49. **Zhang, Y., and J. K. Broome-Smith.** 1990. Correct insertion of a simple plasma-membrane protein into the cytoplasmic membrane of *Escherichia coli*. Gene **96:**51–57.